

# Two Specific Correlation Patterns as Indicators for Various Random Multiplicative Cascade Processes

Wu Yuanfang Wang Yingdan Bai Yuting Liao Hongbo Liu Lianshou

Institute of Particle Physics, Huazhong Normal University, Wuhan 430079 China

FAX: 0086 27 87662646 email: wuyf@iopp.ccnu.edu.cn

## Abstract

It is suggested and demonstrated that two specific 2-dimensional correlation patterns, fixed-to-arbitrary bin and neighboring bin correlation patterns, are efficient for identifying various random multiplicative cascade processes. A possible application of these two correlation patterns to single event analysis in Relativistic Heavy Ion Collider experiments is discussed.

PACS number: 47.27.Eq, 05.40.+j, 47.54.+r, 25.75.Gz

It is well-known that nonlinear phenomena are very popular in nature. Once a set of anomalous scaling law of probability- or “mass”-moments with respect to spatial size [1] is observed in experiment, we recognize that there is self-similar multifractal structure. However, it is difficult to judge what kind of mechanism most likely causes the results since the conventional measures have not provided sufficient information on underlying dynamics. This hinders us from further understanding and studying nonlinear physics. A useful measure for this purpose should not contain too much detail, but enough to capture the essence of production mechanism. In this letter, as a first try along this direction, we will suggest two specific correlation patterns which manifest distinguishable characters of various random multiplicative cascade processes. They will be helpful in exploring the origin of nonlinear and correlation related phenomena.

A random multiplicative cascade process is the simplest example of having a well-defined multifractal structure and has been used extensively in various fields. For example, energy dissipation in fully developed turbulence [1, 2] and successive branchings in QCD parton-shower [3] are both this kind of process and accordingly have multifractal structure. The main idea of such a process is simply a series of self-similar random cascades in spatial partitions. It is generally described as follows: at the first step of the cascade, a given initial interval with length  $\Delta$  and unit probability  $p_0 = 1$  is split into  $\tau$  subdivisions (“bins”). Usually,  $\tau$  is an integer with  $\tau \geq 2$ . The probability for a bin to be split is determined by a weight  $w$  which is distributed according to a splitting function  $p(w_1, w_2, \dots, w_\tau)$ . Then each bin obtained from the first step of the cascade is again independently split into  $\tau$  bins and so on. After  $\nu = 1, 2, \dots, J$  steps, the final number of bins is  $\tau^\nu$ , and the probability in a specific bin  $j_\nu$  is  $\nu$  products of  $w$  over all previous generations:  $p_{j_\nu}^\nu = w_{1j_1} w_{2j_2} \dots w_{\nu j_\nu}$ , where  $j_\mu = 1, 2, \dots, \tau^\mu$  ( $\mu = 1, 2, \dots, \nu$ ). The distribution of  $p_{j_\nu}^\nu$  obtained in this way fluctuates violently from bin to bin, *cf.* Fig. 6 in [1].

By varying the splitting number and/or changing the splitting function, all kinds of random multiplicative cascade processes can be constructed. Especially, an additional physical constraint on the splitting function, like probability conservation at each step of splitting, will cause stronger correlations among the  $\tau$  split bins than those without it. The smaller the splitting number  $\tau$  is,

the stronger are the correlations among the  $\tau$  bins. It is therefore necessary to investigate  $n$ -point correlations in order to probe the differences among the various random cascade processes. Let us start from the simplest 2-point ones.

Why are conventional measurements for 2-point-correlation moments [4] insufficient? This is because they are usually defined at fixed correlation length with both horizontal average over all bins in an event and longitudinal average over all events in a sample. The fixed correlation length makes a comparison between correlations with different scales impossible, and the horizontal average smooths out the differences between different pairs of bins. For these measurements, various random multiplicative processes have the same kind of power law behavior with diminishing correlation length, similar to the scale invariance of “mass” moments. They have little help in the identification of production mechanism. Hence, 2-point correlation moments without horizontal averaging, but with various correlation lengths, are necessary to be presented simultaneously. It should be a *pattern* constructed by all kinds of 2-point correlation moments.

A straightforward pattern of such a kind is the three dimensional pattern of 2-point correlation cumulants [5],

$$C_{K_1, K_2} = \langle \ln p_{K_1} \ln p_{K_2} \rangle_c = \langle \ln p_{K_1} \ln p_{K_2} \rangle - \langle \ln p_{K_1} \rangle \langle \ln p_{K_2} \rangle, \quad (1)$$

where  $K_1$  and  $K_2$  are the coordinates of two points. However, in this pattern the differences among various random multiplicative cascade processes are hidden in complicated background and hard to be observed, *cf.* Fig.1, where the patterns for three different models, the  $\alpha$  model without probability conservation [4], the  $p$  model with probability conservation [6] and the  $c$  model with both probability conservation and random probability partition at each step of the splitting [7], are presented. The pattern manifests the common characteristics of random multiplicative cascade processes, such as symmetry at each step of splitting, the largest correlations of any bin with itself and so on, but is insensitive to the basic model assumptions. Thus, it is better to present the correlations of some specific two bins in a two dimensional pattern so that the differences in various processes are manifested.

A simple way to do so is to fix one bin  $K_1$  and vary the left one  $K_2$ . It is a fixed-to-arbitrary bin correlation pattern. It contains correlation information at various lengths from the fixed bin to all other bins, in which  $\tau - 1$  bins are separated from the fixed one at the last cascade step and  $\tau^J - \tau$  bins are separated successively from the fixed one before the last step of cascading. Another simple way is to fix the distance between the two bins and change the position of them. Since the correlations among  $\tau$  bins at each step of splitting are important information, the distance between two bins are better to be as close to each other as possible, *i.e.*  $K_1 = K$  and  $K_2 = K + 1$ , where  $K = 1, 2, \dots, \tau^J - 1$ . This is a neighboring bin correlation pattern. These two correlation patterns provide useful information on cascade mechanism and filter out the common characteristics of random multiplicative cascade processes.

In the following, as a support of above arguments, the correlation cumulants for three different random cascade processes, the  $\alpha$ , the  $p$  and the  $c$  models, are first derived in order to show how the different appearances of these cumulants are caused by the model assumptions. Then it is argued and demonstrated why the measurements for these two patterns provide information on the model assumptions. Finally, the extension and application of the patterns are discussed.

These three models are examples of the random binary cascade processes with symmetric splitting functions  $p(w_1, w_2) = p(w_2, w_1)$ . In this case, Eq.(1) can be written simply as [5]

$$C_{K_1, K_2} = A(J - d_2) + B(1 - \delta_{d_2, 0}), \quad (2)$$

where  $d_2 = J - \sum_{j=1}^J \delta_{k_1^1, k_1^2} \cdots \delta_{k_j^1, k_j^2}$  is the ultrametric distance, which is a measure of how many generations one has to move up before a common ancestor is found;

$$A = \partial^2 Q[\lambda_1, \lambda_2] / \partial \lambda_1^2 |_{\lambda=0}, \quad B = \partial^2 Q[\lambda_1, \lambda_2] / \partial \lambda_1 \partial \lambda_2 |_{\lambda=0} \quad (3)$$

are respectively the so called ‘‘same-lineage’’ cumulant, which is the correlation of the common ancestor of  $K_1$  and  $K_2$ , and the ‘‘splitting’’ cumulant, which measures the correlation between the two parts split first from their common ancestor;

$$Q[\lambda_1, \lambda_2] = \ln \left[ \int dw_1 dw_2 p(w_1, w_2) \exp(\lambda_1 \ln w_1 + \lambda_2 \ln w_2) \right] \quad (4)$$

is the branching generating function (BGF).

For the  $\alpha$  model, the  $w_1$  or  $w_2$  at each step of splitting is two possible numbers,  $1 + \alpha$  and  $1 - \alpha$ , with equal probability for each of them. Hence, its splitting function [5] can be written as:

$$p(w_1, w_2) = \frac{1}{4} \left[ \delta(w_1 - (1 + \alpha)) + \delta(w_1 - (1 - \alpha)) \right] \left[ \delta(w_2 - (1 + \alpha)) + \delta(w_2 - (1 - \alpha)) \right], \quad (5)$$

where  $\alpha$  is a fixed parameter in the region  $[-1, 1]$ . Inserting this function into Eq.(4) and then Eq.(4) into Eq.(3), the “same-lineage” and the “splitting” cumulants can be easily derived:

$$A_\alpha = \frac{1}{4} \left[ \ln \frac{1 + \alpha}{1 - \alpha} \right]^2, \quad B_\alpha = 0. \quad (6)$$

$B_\alpha = 0$  means that there is no correlation between the two parts for every splitting. This is due to the independence of  $w_1$  and  $w_2$  assumed in the model.

For the  $p$  model, the summation of  $w_1$  and  $w_2$  keeps to be 2, with  $w_1 = 1 \pm \beta$  and  $w_2 = 1 \mp \beta$  as the consequence of probability conservation, here  $\beta$  is a fixed parameter in the region  $[-1, 1]$ . Its splitting function [5] is

$$p(w_1, w_2) = \frac{1}{2} \left[ \delta(w_1 - (1 + \beta)) + \delta(w_1 - (1 - \beta)) \right] \delta(w_1 + w_2 - 2), \quad (7)$$

and its “same-lineage” and “splitting” cumulants are

$$A_p = \frac{1}{4} \left[ \ln \frac{1 + \beta}{1 - \beta} \right]^2, \quad B_p = -\frac{1}{4} \left[ \ln \frac{1 + \beta}{1 - \beta} \right]^2. \quad (8)$$

Due to probability conservation, the “splitting” cumulant  $B$  has sign opposite to the “same-lineage” cumulant  $A$ . Moreover, since  $\beta$  is a unique fixed number, the derivatives of BGF with respect to one of the two  $\lambda$ 's twice are equivalent to those with respect to both of them. This is why the absolute value of the “same-lineage” cumulant  $A$  is equal to that of the “splitting” cumulant  $B$ .

For the third  $c$  model,  $w_1 + w_2 = 1$  similar to the  $p$  model. Distinct from the  $p$  and the  $\alpha$  models, the weight  $w$  is allowed to be a random number *e.g.*  $w_1 = (1 + \gamma r)/2$  and  $w_2 = (1 - \gamma r)/2$ , here  $r$  is a random number uniformly distributed in the interval  $[-1, 1]$  and  $\gamma$  is a fixed model parameter in

the region  $[0, 1]$ . Obviously, this model is more flexible and closer to the real system with probability conservation. The splitting function is:

$$p(w_1, w_2) = \frac{1}{\gamma} \left[ \theta \left( w_1 - \frac{1-\gamma}{2} \right) - \theta \left( w_1 - \frac{1+\gamma}{2} \right) \right] \delta(w_1 + w_2 - 1). \quad (9)$$

and its “same-lineage” and “splitting” cumulants are:

$$A_c = \frac{1}{\gamma} \int_{\frac{1-\gamma}{2}}^{\frac{1+\gamma}{2}} (\ln w_1)^2 dw_1 - \frac{1}{\gamma^2} \left[ \int_{\frac{1-\gamma}{2}}^{\frac{1+\gamma}{2}} \ln w_1 dw_1 \right]^2, \quad (10)$$

$$B_c = \frac{1}{\gamma} \int_{\frac{1-\gamma}{2}}^{\frac{1+\gamma}{2}} \ln w_1 \ln(1-w_1) dw_1 - \frac{1}{\gamma^2} \left[ \int_{\frac{1-\gamma}{2}}^{\frac{1+\gamma}{2}} \ln w_1 dw_1 \right]^2. \quad (11)$$

The “splitting” cumulant is nonzero due to probability conservation. The absolute values of the “same-lineage” and the “splitting” cumulants are unequal since  $w_1$  and  $w_2$  are no longer fixed to a particular number, unlike the  $p$  model.

From the above analytic derivation, we see that the three random cascade models are very different in the absolute values of their “splitting” cumulants and in the relative values of these cumulants to the “same lineage” cumulants. These differences are due to the basic model assumption and independent of the model parameters. Therefore, a useful 2-point correlation pattern should contain information on the “splitting” cumulant and its relation to the “same lineage” cumulant. This requirement turns out to be two possible combinations of the coefficients  $A$  and  $B$  in Eq.(2): (1)  $C_{K_1, K_2} = B$ , *i.e.*  $J - d_2 = 0$  and  $1 - \delta_{d_2, 0} = 1$ ; (2)  $C_{K_1, K_2} = A + B$ , *i.e.*  $J - d_2 = 1$  and  $1 - \delta_{d_2, 0} = 1$ ; for the first combination,  $d_2 = J$  and  $d_2 \neq 0$  means that common ancestor has to be at the initial interval if  $J > 0$ . The fixed-to-arbitrary bin correlation pattern happens to have  $2^{J-1} \cdot (2-1)$  pairs of this kind of bins. The neighboring bin correlation pattern also has a pair of this kind of bins at center  $K = 2^{J-1}$ . For the second combination,  $d_2 = J - 1$  and  $d_2 \neq 0$  implies that common ancestor locates at the first cascade step. In the fixed-to-arbitrary bin correlation pattern,  $2^{J-2} \cdot (2-1)$  pairs of bins have common ancestor at the first cascade step. The neighboring bin correlation pattern again has two pairs of such a kind of bins at  $K = 2^{J-2}$  and  $K = 2^{J-2} \cdot 3$  respectively. Hence the suggested two correlation patterns are useful measures in identifying the above mentioned three random cascade processes.

We first plot the fixed-to-arbitrary bin correlation pattern for the  $\alpha$ , the  $p$  and the  $c$  models in Figs. 2(a), (b) and (c), respectively, with the model parameters  $\alpha = 0.4$ ,  $\beta = 0.4$ ,  $\gamma = 0.8$ ,  $J = 6$ . The ordinate is the correlation strength  $C_{1,K_2}$ ; the abscissa is the bin  $K_2$  which varies as  $K_2 = 2, 3, \dots, 64$ , and the fixed bin is located at  $K_1 = 1$ . Since the larger the distance between the two bins is, the earlier the two bins are separated in cascade process, the correlation strength decreases as the arbitrary bin  $K_2$  goes further away from the fixed one  $K_1$ . The number of points with the same height or same correlation strength increases as  $2^{\nu-1} \cdot (2-1)$  with  $\nu = 1, 2, \dots, J$ . The number 2 comes from the binary cascade. Generally, it is  $\tau^{\nu-1} \cdot (\tau-1)$ . So by counting the number of points in each correlation strength, the splitting number of the cascade process can be estimated.

The possible correlation strengths in these three models are different: (1) the weakest one in the  $\alpha$  model is zero; (2) there are both zero and negative ones in the  $p$  model; (3) negative ones, but no zero ones, are allowed in the  $c$  model. These differences come from the different model assumptions. The absence of negative correlations implies independent splitting in the model,  $B = 0$ , such as is the case for the  $\alpha$  model. If there are both negative and zero correlations in the pattern, the positive one from the “same-lineage” cumulant  $A$  must be equal to the negative one from the “splitting” cumulant  $B$ . So that  $B < 0$  for the weakest one and  $A + B = 0$  for the following one, as for the  $p$  model. Having negative, but no zero, correlation, means that the “same-lineage” cumulant is different from the “splitting” cumulant, or  $A + B \neq 0$  and  $B < 0$ , as for the  $c$  model.

The neighboring bin correlation pattern  $C_{K,K+1}$  with  $K = 1, 2, \dots, 2^J - 1$  can show us the same thing. In Fig.3, the patterns for the three models are presented. Here, the strongest correlations are of those two neighboring bins split at the last step of cascade, *i.e.*,  $K = 1, 3, \dots, 2^J - 2^0$ ; the next ones happen to be of those split before the last step of cascade, *i.e.*,  $K = 2, 6, 10, \dots, 2^J - 2^1$ ; and so on. The number of points at a certain correlation strength is determined by  $2^{\nu-1}$ , or  $\tau^{\nu-1}$  in general, with  $\nu = J, J-1, \dots, 1$ . There are only positive and zero correlation spectra in the  $\alpha$  model. In the  $p$  model, the correlation spectrum ranges over positive, zero and negative values, while for the  $c$  model, only positive and negative correlations are allowed with no zero ones.

Therefore, from the measurements of these two correlation patterns, we can find out by what

kind of random multiplicative cascade process the observed system are produced. This is a first step toward the revelation of underlying mechanism of multifractal phenomena. The extension of these two patterns to the mixture of different random cascade processes and other mechanisms, which can lead to multifractal structure, is obviously the next step. Their corresponding patterns will not be so regular as those of the above mentioned three processes. For the further identification of the production mechanism in general, other measures may be needed in addition to these two. Nevertheless, having established these two patterns for some known mechanisms, it is interesting to compare the patterns measured in practice with them and judge if there are similar generating mechanism.

A possible application of these two correlation patterns is in the single event analysis of Relativistic Heavy Ion Collider (RHIC) experiments [8]. In these experiments, the probability of final state particles falling into a particular bin in rapidity or pseudo-rapidity can be well estimated by [9],  $p_{K_i} \approx n_{K_i}/N$ , where  $n_{K_i}$  is the number of final state particles falling into the  $K_i$ -th bin and  $N$  is the total number of particles in the event, which is typically several thousand [10]. At the current experimental resolution in rapidity, there is almost no empty bin. In this case, it is much better to investigate directly the pattern of a single event without averaging over all events in the sample. The 2-point correlation cumulant for a single event can be defined as:

$$C_{K_1, K_2}^{(e)} = \ln p_{K_1} \ln p_{K_2} - \langle \ln p_{K_1} \rangle \langle \ln p_{K_2} \rangle, \quad (12)$$

its average over all events in a sample equals to the 2-point correlation cumulant  $C_{K_1, K_2}$  of Eq.(1). The whole event sample can then be classified by the measured correlation patterns of single event. Some events which have undergone a phase transition to Quark Gluon Plasma (QGP) will most likely have very special patterns, since during this transition, all kinds of correlations, the long as well as the short ones, will change dramatically.

In this letter, we investigate two specific 2-dimensional correlation patterns: the fixed-to-arbitrary bin and the neighboring bin correlation patterns. The former shows correlations at various lengths, and the latter has short-range correlations at different positions. They are sensitive to the underlying



mechanisms and work equally well in identifying various random multiplicative cascade processes. As an example, their application to the analysis of single event of current Relativistic Heavy Ion Collider(RHIC) experiments has been discussed. For more-than-2-point correlations, we can also find some useful correlation patterns in a similar way. The measurements for all of them will hopefully open a new world in the research of nonlinear and correlation related physics.

We are grateful for the helps of Dr. Jimmy MacNaughton in the presentation of the paper and the good suggestions of Dr. Nu Xu. This work is supported in part by the SFC under project 90103019; Cross-century Talent Foundation of National Education Committee of China under Grant No.1 [1998].

## References

- [1] G. Paladin and A. Vulpiani, *Phys. Reports* **4** (1987).
- [2] B. Mandelbrot, *J. Fluid. Mech.* **62**, 331(1974); U. Frisch, P. Sulem and M. Nelkin, *J. Fluid. Mech.* **87**, 719(1978); S. Lovejoy and D. Schertzer in Proc. Conf. Turbulent Shear Flows 4, eds. L. J. S. Bradbury *et al.* (Springer, Berlin, 1984) and references therein.
- [3] R. P. Feynman, Proc. 3rd Workshop on Current Problems in High Energy Particle Theory, Florence, 1979, eds. R. Casalboni *et al.*, Johns Hopkins University Press, Baltimore, 1979; G. Veneziano, *ibid.* p.15; K. Konishi, A. Ukawa and G. Veneziano, *Phys. Lett. B* **78**, 243(1978); *Nucl. Phys. B* **157**, 45(1979).
- [4] A. Białas and R. Peschanski, *Nucl. Phys. B* **308**, 857(1988); P. Bożek, M. Płoszajczak, R. Botet, *Phys. Reports* **252**, 101(1995).
- [5] Martin Greiner, Hans C. Eggers and Peter Lipa, *Phys. Rev. Lett.* **80**, 5333(1998); M. Greiner, J. Schmiegel, F. Eickemeyer, P. Lipa and H. C. Eggers, *Phys. Rev. E* **58**, 554(1998).
- [6] C. Meneveau and K. R. Sreenivasan, *Phys. Rev. Lett.* **59**, 1424(1987).
- [7] Wu Yuanfang and Liu Lianshou, *Phys. Rev. Lett* **70**, 3197(1993).
- [8] Harris J. W., *Nucl. Phys. A***566**, 277(1994).
- [9] Wu Yuanfang and Liu Lianshou, *Phys. Rev. D* **43**, 3077(1991); Fu Jinghua, Wu Yuanfang and Liu Lianshou, *Phys. Lett. B* **472**, 161(2000).
- [10] B. B. Back *et al.*, *Phys. Rev. Lett.* **85**, 3100(2000).

## Figure Captions

**Fig.1** The correlation cumulants  $C_{K_1, K_2}$  of (a) the  $\alpha$  model, (b) the  $p$  model and the (c)  $c$  model.

**Fig.2** The fixed-to-arbitrary bin correlation patterns  $C_{1, K_2}$  of (a) the  $\alpha$  model, (b) the  $p$  model and (c) the  $c$  model, where the ordinate is correlation strength  $C_{1, K_2}$  and the abscissa is  $K_2 = 2, 3, \dots, 64$ . The solid lines in the figures indicate zero correlation strength.

**Fig.3** The neighboring bin correlation patterns  $C_{K, K+1}$  of (a) the  $\alpha$  model, (b) the  $p$  model and (c) the  $c$  model, where the ordinate is correlation strength  $C_{K, K+1}$  and the abscissa is  $K = 1, 2, \dots, 63$ . The solid lines in the figures indicate zero correlation strength.

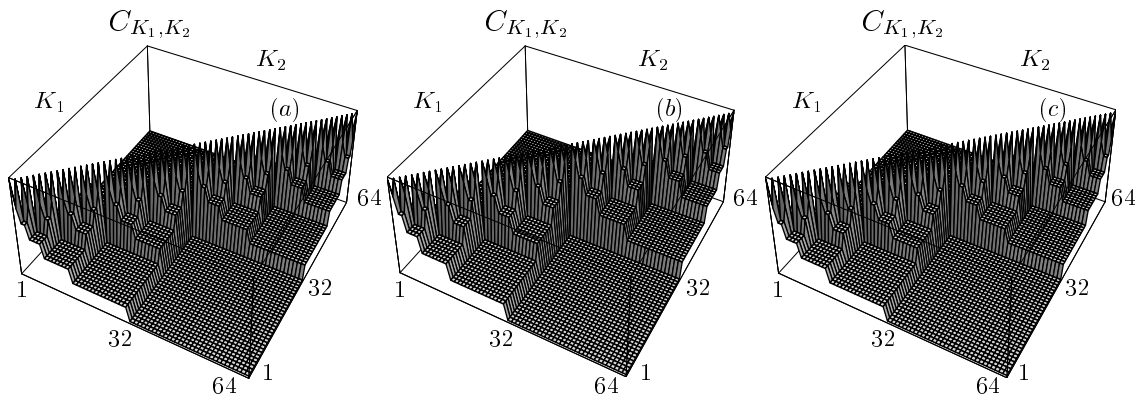


Fig.1

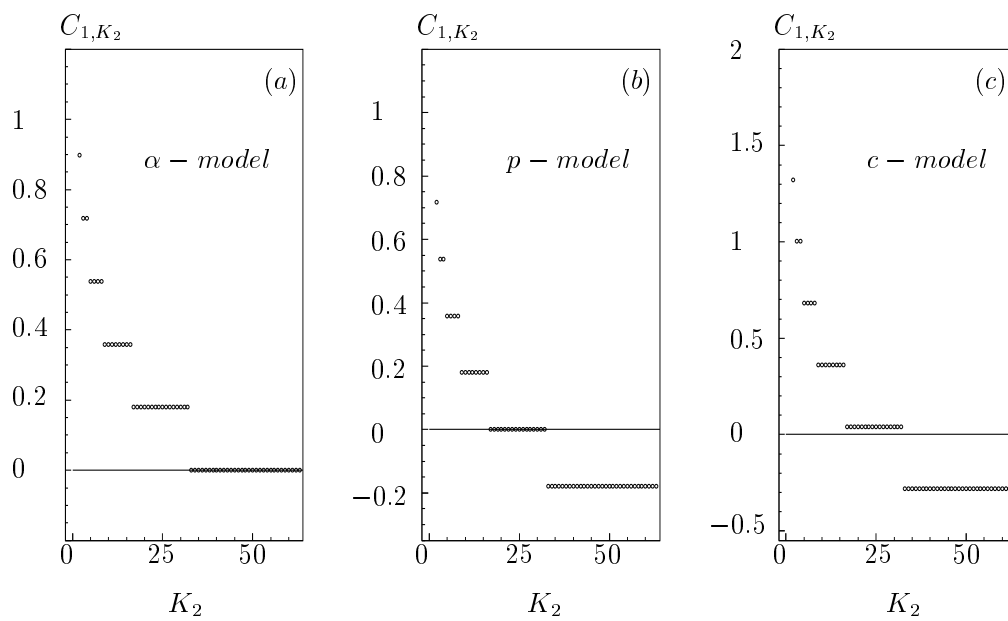


Fig.2

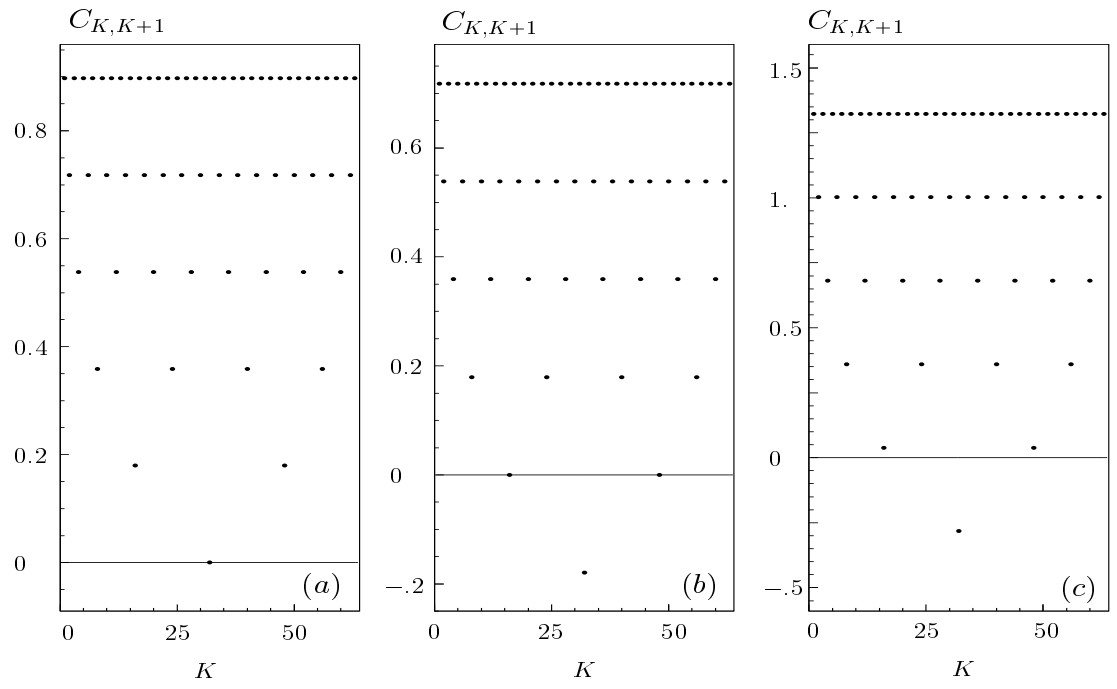


Fig.3